COMSOL CONFERENCE 2024 FLORENCE

Impact of Battery Operation and Manufacturing Process on Battery Performance over Lifetime

T. Bisgaard[1,*], A.G. Steckel[1], M.R. Nielsen[1]
1. Resolvent Denmark PS, Maaloev, Denmark.
* Corresponding author: tb@resolvent.dk

Abstract
Batteries are a crucial technology enabler towards climate neutrality, and there is an urgent need to improve resource efficiency while transitioning to next-generation technologies. A mechanistic battery model can accelerate this development by guiding battery design and optimization alongside experimentation. This work highlights the integration of a degradation mechanisms in the Doyle-Fuller-Newman pseudo-2D framework. The model successfully captures the trend of all employed data using a single fitted parameter set. Such a rigorous simulation-based approach ensures applicability across conditions, supporting the creation of surrogate models for efficient, high-fidelity battery pack simulations.
Keywords: Lithium ion, degradation, battery, cell, cycling, electrochemistry.

Introduction
Global Lithium-ion battery demand is expected to grow 27% annually to 4700 GWh by 2030 [1]. Growing battery applications are within mobility such as electric vehicles (EVs) and battery energy storage systems (BESS). Battery pack efficiency, longevity, recyclability are critical design targets to meet sustainability targets, which also entails responsible use of essential raw materials such as Lithium and Nickel. High fidelity simulation is needed to support the technology development to increase raw material utilization and shorten time to market of new developments.

Electrochemistry in Batterise
Models for liquid electrolyte batteries with intercalating electrodes are well developed, with the Doyle-Fuller-Newman (DFN) model among the most used formulations [2]. A conventional current collector. electrode, separator, electrode, current collector sandwich (Figure 1) can be described via Li-ion transport, electric current, ionic current transport, and heat conduction.

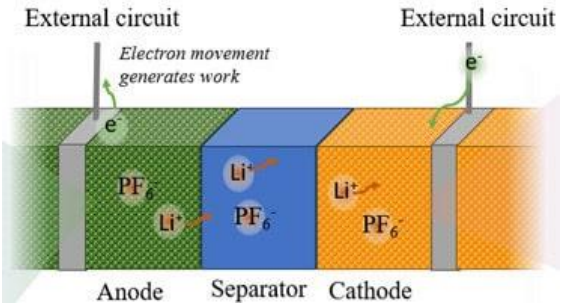

Figure 1. Liquid Electrolyte Lithium Ion Battery.

The electrode domains are treated as homogeneous when it comes to Li-ion transport but are described by an additional dimension representing the radius of the electrode particles within the electrode domain. Hence, describing the battery domain in 1D, incorporating the radial dimension increases the dimension by one, thereby arriving at the common term “pseudo 2D”. Li-ions in the electrolyte solution act as charge carriers and transfer freely in the electrolyte solution. Table 1 summarizes the relevant physics across the different domains. The following sections will describe the “electrode diffusion” and “reaction” phenomena in more detail.

Table 1. Physics in LIB Domains.

Phenomena	Current collector	Anode	Separator	Cathode	Current collector
Li-ion diffusion	-	×	×	×	-
Electric Current	×	×	-	×	×
Ionic current	-	×	×	×	-
Electrode diffusion	-	×	-	×	-
Reaction	-	×	-	×	-
Heat conduction	×	×	×	×	×

Intercalation
Intercalation is the insertion of Li-ion into a layered material, such as the electrode materials. The rate of intercalation is given by the current density following Butler-Volmer expression (Eq- 1).

$$i_{int,j} = i_{int0,j}\left[\exp\left(\frac{\alpha\mathcal{F}\eta_{int,j}}{RT}\right) - \exp\left(-\frac{(1-\alpha)\mathcal{F}\eta_{int,j}}{RT}\right)\right]$$

Eq- 1

$j \in [n, s, p]$ denotes the negative electrode (anode), separator, and positive electrode (cathode), respectively.
The intercalation overpotential $\eta_{int,j}$ and the rate constant $i_{0,j}$ are given by Eq- 2 and Eq- 3, respectively.

$$\eta_{int,j} = \phi_{S,j} - \phi_{E,j} - U_{0,j} - i_{tot,j}R_f$$

Eq- 2

$$i_{int0,j} = k_{int,j}\left(\frac{c_{E,j}}{c^{ref}}\right)^{1-\alpha}\left(\frac{c_{S,max,j} - c_{S,j}}{c_{S,max,j}}\right)^{1-\alpha}\left(\frac{c_{S,j}}{c^{ref}}\right)^{\alpha}$$

Eq- 3

Here $c^{ref} = 1[mol\ m^{-3}]$ to ensure consistent units.

An Arrhenius-type expression is introduced to capture temperature dependency of the rate constant according to Eq- 4.

$$k_{int,j} = k_{int,j,ref}\exp\left[-A_{int,j}\left(\frac{1}{T_{ref}} - \frac{1}{T}\right)\right]$$

Eq- 4

Electrode Particle Inventory
An essential concept in the DFN is the incorporation of diffusion in particles of well-defined geometries. In this work, spherical particles are used. Li (in anode) and Li-ions (in cathode) diffusion in spherical particles are given by Eq- 5 with boundary conditions in Eq- 6 and Eq- 7.

$$\frac{\partial c_{S,j}}{\partial t} = \frac{1}{r^2}\frac{\partial}{\partial r}\left(r^2 D_{eff,S,j}\frac{\partial c_{S,j}}{\partial r}\right)$$

Eq- 5

$$\left(-4\pi r^2 D_{eff,S,j}\frac{\partial c_{P,j}}{\partial r}\right)\Big|_{r=\delta_{P,j}} = -4\pi\delta_{P,j}^2\frac{1}{\mathcal{F}}i_{tot,j}$$

Eq- 6

$$\frac{\partial c_{P,j}}{\partial r}\Big|_{r=0} = 0$$

Eq- 7

Again, Arrhenius type expression is employed for the temperature dependency of diffusion coefficient according to Eq- 8.

$$D_{eff,S,j} = D_{eff,S,j,ref}\exp\left[-B_{eff,j}\left(\frac{1}{T_{ref}} - \frac{1}{T}\right)\right]$$

Eq- 8

The total current density i_{tot} is given by Eq- 9.

$$i_{tot} = i_s + i_{int}$$

Eq- 9

i_s is the current density of the degradation process, which is described in the following subsection.

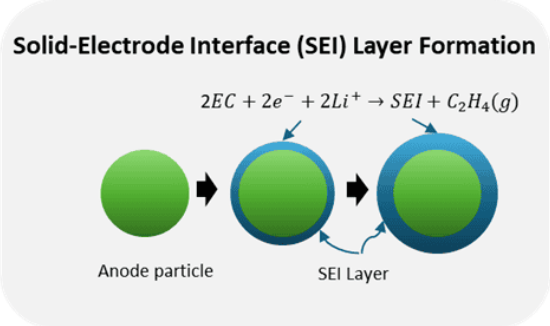

Figure 2. Degradation Model Illustration.

Degradation – SEI Layer Formation
Electrical capacity will inevitably decrease over time for a LIB while internal resistance increases due to several degradation mechanisms depending on its historical conditions. Some important factors are temperature, state of charge, and load profile. Consequently, both capacity loss and power loss are observed over time. SEI formation is considered the primary degradation mechanism during the first charge/discharge cycles of a battery.
The SEI formation can be modelled using the approach of Safari et al. [3]. In this approach, solvent (ethyl carbonate, EC) diffuses through the SEI layer and reacts with electrode particles on the interface, from where new SEI layer is formed. In this process, both solvent and Lithium are consumed following reaction scheme Eq- 10 (see Figure 2).

$$2EC + 2e^- + 2Li^+ \rightarrow SEI + C_2H_4(g)$$

Eq- 10

A mass balance of solvent in SEI Layer is governed by diffusion and convection according to Eq- 11 with boundary conditions Eq- 12 and Eq- 13. Convection is caused by SEI layer growth.

$$\frac{\partial c_{EC,P}}{\partial t} = \frac{\partial}{\partial r}\left(D_{EC,P}\frac{\partial c_{EC,P}}{\partial r}\right) - \frac{d\delta_{SEI}}{dt}\frac{\partial c_{EC,P}}{\partial r}$$

Eq- 11

$$c_{EC,P}\big|_{r=\delta_{P,j}+\delta_{SEI}} = \varepsilon_{SEI}c_{EC,\infty}$$

Eq- 12

$$\left(-D_{EC,P}\frac{\partial c_{EC,P}}{\partial r} + \frac{d\delta_{SEI}}{dt}c_{EC,P}\right)\Big|_{r=\delta_{P,j}} = \frac{i_s}{F}$$

Eq- 13

Here using $\varepsilon_{SEI} = 0.5[-]$ [3]. As $\delta_{SEI} \ll \delta_{P,n}$ the particle curvature can be neglected.
The growth rate of the SEI layer follows Eq- 14 with boundary condition Eq- 15.

$$\frac{d\delta_{SEI}}{dt} = -\frac{i_s}{2\mathcal{F}}\frac{M_{SEI}}{\rho_{SEI}}$$

Eq- 14

$$\delta_{SEI}|_{t=0} = \delta_{SEI,init}$$

Eq- 15

One half (½) mole of SEI layer is produced per mole of electrons and per mole of Li-ions consumed according to Eq- 10.
The SEI layer formation current density follows Eq- 16.

$$i_s = -\mathcal{F} k_{f,s} c_{EC,surf} \exp\left[-\frac{\beta\mathcal{F}}{RT}\left(\phi_{S,n} - \frac{\delta_{SEI}}{\kappa_{SEI}} i_{tot}\right)\right]$$

Eq- 16

To summarize, solvent component ethylene carbonate (EC) diffuses through the continuously growing SEI layer to form new SEI layer material on the anode particle surface.

Coupling of Domains

The 1D battery domain only "sees" the particle surface concentrations of Lithium from the 2D domain (Eq- 17).

$$c_{S,surf,j}(x) = c_{P,j}(x,r)\big|_{r=\delta_{P,j}}$$

Eq- 17

The same applies to the degradation reaction of EC at the electrode particle surface (Eq- 18).

$$c_{EC,surf}(x) = c_{EC,P}(x,r)\big|_{r=\delta_{P,j}}$$

Eq- 18

The surface Lithium concentration ($c_{S,surf,j}(x)$) is also used to calculate the half-cell potentials of the electrodes.

Derived Variables

Using the dependent field variables c_E, c_S, ϕ_E, ϕ_S, δ_{SEI}, and T resulting from simulation, the battery performance can be quantified and analyses. We define the average particle saturation, which corresponds to the equilibrium concentration of an open cell battery for $t \to \infty$. The average particle saturation is given by Eq- 19.

$$\theta_{avg,j}(x) = \frac{\int_{r=0}^{\delta_{P,j}} 4\pi r c_{P,j}(x,r)dr}{\int_{r=0}^{\delta_{P,j}} 4\pi r dr} = \frac{\int_{r=0}^{\delta_{P,j}} 4\pi r c_{P,j}(x,r)dr}{\frac{4}{3}\pi\delta_{P,j}^3}$$

Eq- 19

We define the depth of discharge (DOD) based on the cathode (Eq- 20).

$$DOD = \frac{\frac{1}{L_p}\int_{x=L_{cell}-L_p}^{L_p} \theta_{avg}(x,r)dr}{\theta_{max,S,p} - \theta_{min,S,p}}$$

Eq- 20

The state of charge (SOC) is defined as via the DOD according to Eq- 21.

$$SOC = 1 - DOD$$

Eq- 21

The C-rate is defined as a full charge/discharge of the cathode in one hour according to Eq- 22.

$$I_{1C} = \frac{L_p A_{cell} \varepsilon_{S,p} c_{S,max,p}(\theta_{max,p} - \theta_{min,p})}{3600[s]}$$

Eq- 22

Note that the electrode capacity should be balanced [4]. In this work, the cathode is the limiting electrode.

Summary

We have briefly described the governing equations for modelling the dynamics of Lithium transport and degradation in electrode particles. The presented model accounts for:

- Loss of lithium inventory
- Internal resistance
- SOC
- Input current
- Temperature

Numerical Simulation

The DFN model including the degradation model, described in the previous subsection, were implemented in COMSOL Multiphysics 6.1 using custom Coefficient PDE Interfaces (Partial Differential Equations).
As described earlier, a 1D domain is used to represent the sandwich of battery layers using x as the spatial dimension. For Lithium diffusion in particles, 2D domains were used to include the additional radial dimension (r). The physics in all domains are solved simultaneously using the couplings features (i.e., Extrusion) in COMSOL as inspired by Cai and White [5]. The coupling of the two domains is illustrated in Figure 3.

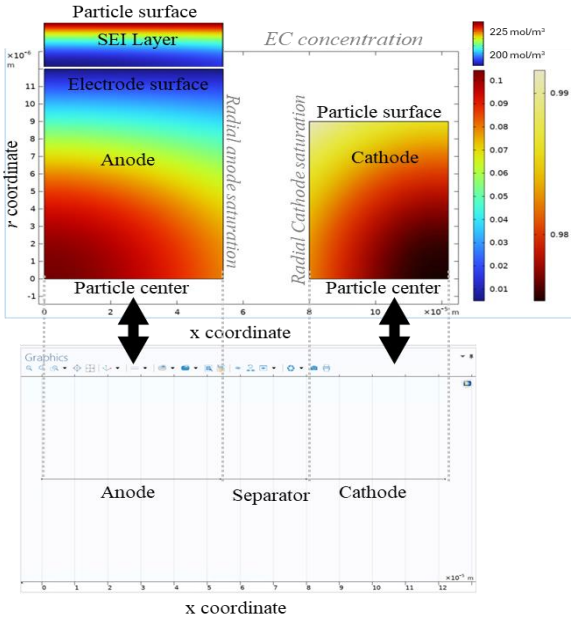

Figure 3. Coupling of 1D and 2D Domains.

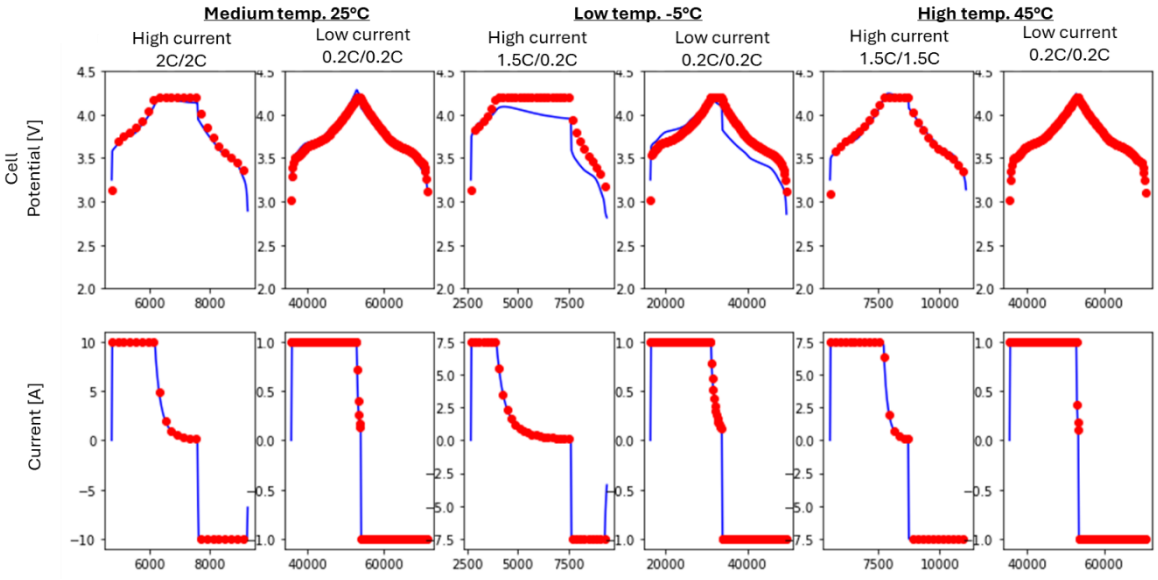

Figure 4. Top row: Battery Cell Potential versus Time. Bottom row: Current versus Time. Blue: Best Fit Simulation, i.e., one common parameter set. Each column corresponds to different conditions. Red: Experimental Data (resampled).

The 2D domain of the SEI layer can be represented by the anode particle domain using the displaced radial coordinate $\bar{r}$ according to Eq- 23.

$$\bar{r} = \frac{r - \delta_{P,n}}{\delta_{SEI}} \delta_{P,n}$$

Eq- 23

Note that $\bar{r} \in [0; \delta_{P,n}]$, which spans the same range as the anode particle r coordinate.

Using chain rule, the model (Eq- 11, Eq- 12, and Eq- 13) can be reformulated as Eq- 24 with boundary conditions Eq- 25 and Eq- 26.

$$\frac{\delta_{SEI}(t)}{\delta_0}\frac{\partial c_{EC,P}}{\partial t} + \frac{\partial}{\partial \bar{r}}\left(-\frac{\delta_0 D_{EC,P}}{\delta_{SEI}(t)}\frac{\partial c_{EC,P}}{\partial \bar{r}} + \frac{d\delta_{SEI}}{dt} c_{EC,P}\right) = 0$$

Eq- 24

$$c_{EC,P}|_{\bar{r}=\delta_{P,n}} = \varepsilon_{SEI} c_{EC,\infty}$$

Eq- 25

$$\left(-\frac{\delta_{P,n} D_{EC,P}}{\delta_{SEI}}\frac{\partial c_{EC,P}}{\partial \bar{r}} + \frac{d\delta_{SEI}}{dt} c_{EC,P}\right)|_{\bar{r}=0} = \frac{i_s}{F}$$

Eq- 26

Case Studies

Parameter Fitting and Validation

Battery cell data at different conditions were obtained from https://www.batteryarchive.org/. Sequential parameter fitting was performed, starting from a fresh battery cell using 6 data sets (high /medium /low temperature at high /low discharge C-rate, isothermal conditions) followed by cycling of a battery cell using 2 data sets (medium /low temperature at medium discharge C-rate). The Arrhenius parameters for temperature dependency for reaction kinetics ($k_{int,j,ref}$ and $A_{int,j}$ in Eq- 4) and diffusion coefficients ($D_{eff,s,j,ref}$ and $B_{eff,j}$ Eq- 8) for anode and cathode were used as fitting parameters.

COMSOL Application Builder was used to load data series experimental points, calculate squared mean error of battery cell potential, and to export the simulated time series data. An excellent fit was obtained across all datasets with a squared mean error of $0.012[V^2]$ for fresh battery cell. The potential and current profiles for the different data sets are illustrated in Figure 4.

After fixing the fresh battery parameters, the degradation parameters were fitted based on two time series data sets (medium /high temperature at medium discharge C-rate). The adjustable parameters were $k_{f,s}$ in Eq- 16 and $D_{EC,P}$ in Eq- 24. Again, an excellent fit was obtained with an acceptable squared mean error of $0.667[V^2]$ for the cycled battery cell. A comparison of achieved discharge energy for the first 75 cycles in simulation compared to experimental values is illustrated in Figure 5. Starting from an initial uniform SEI layer thickness of $\delta_{SEI,init} = 5[nm]$, the average thickness has grown to 48[nm] after 75 cycles and in accordance with the trend of Figure 6. Finally, a data set at -5[°C] and discharge/charge 2C-Rate was used for validation (see Figure 7). Yet again, an acceptable result is achieved. However, as the experimental current is input for simulation, difficulties in achieving identical constant potentials at cut-off points are expected.

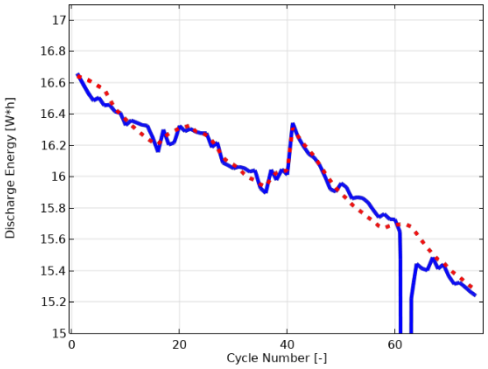

Figure 6. Discharge Energy versus Cycle Number. Blue: Simulation. Red: Experimental Data.

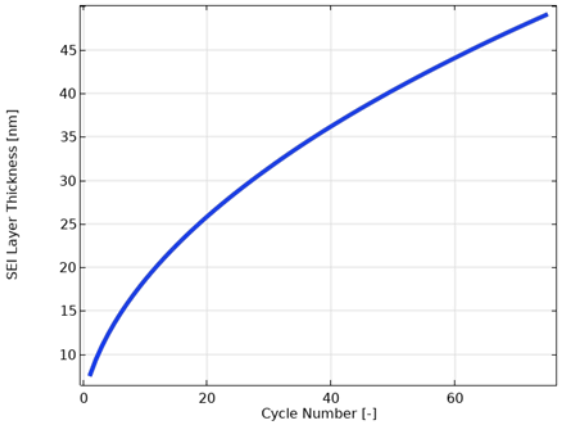

Figure 5. Average SEI Layer Thickness.

Conclusions

This work incorporates degradation mechanisms through COMSOL's custom PDE interfaces within the Doyle-Fuller-Newman pseudo-2D framework, offering a robust simulation-based method for both battery cell and pack design. Its adaptability across varying conditions promotes resource-efficient optimization and aids the advancement of next-generation technologies. Additionally, the model benefits from a reliable parameter fitting framework, allowing for accurate tuning of battery parameters, including temperature effects.

References

[1] McKinsey, "Battery demand is growing-and so is the need for better solutions along the value chain," Alliance, McKinsey's Battery Accelerator Team and Global Battery, 16 January 2023. [Online]. Available: www.mckinsey.com. [Accessed September 2024].

[2] M. Doyle, T. Fuller and J. Newman, "Modelling the Galvanostatic Charge and Discharge of the Lithium/Polymer/Insertion Cell," *Journal of the Electrochemical Society*, vol. 140, no. 6, p. Preprint, 1992.

[3] M. Safari, M. Morcrette, A. Teyssot and C. Delacourt, "Multimodal Physics-Based Aging Model for Life Prediction of Li-Ion Batteries," *Journal of The Electrochemical Society - J ELECTROCHEM SOC*, vol. 156, no. 3, pp. A145-A153, 2009.

[4] H. Ekström, "COMSOL Blog," 16 May 2019. [Online]. Available: www.comsol.com/blogs. [Accessed September 2024].

[5] L. Cai and R. White, "Mathematical Modeling of a Lithium Ion Battery," *Excerpt from the Proceedings of the COMSOL Conference 2009 Boston*, 2009.

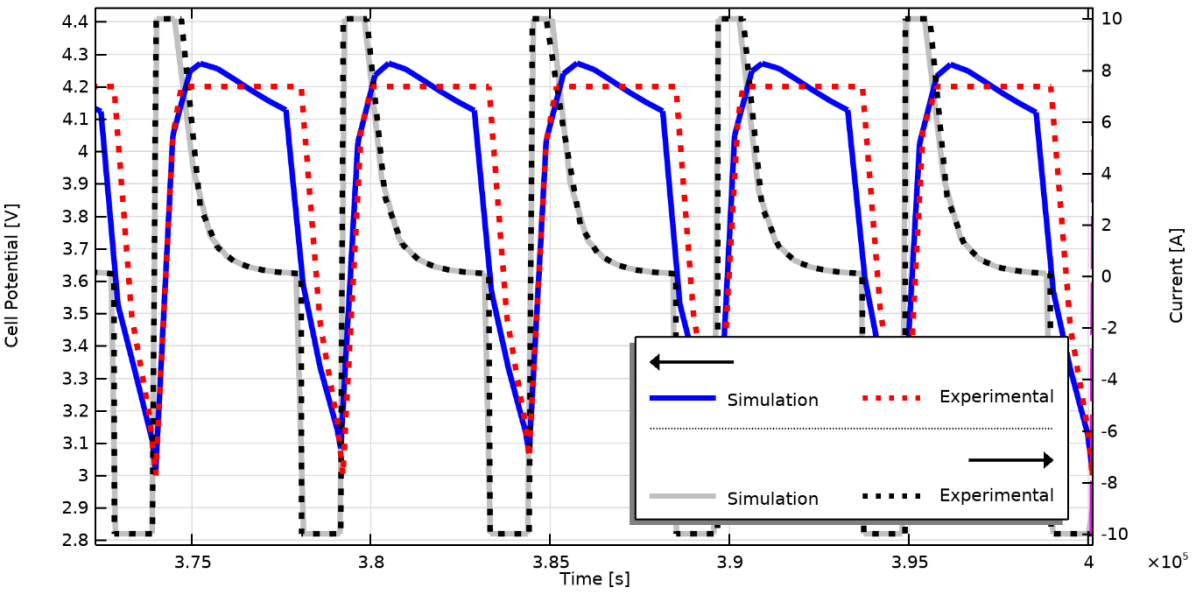

Figure 7. Comparison of Simulation and Experimental Data for Validation set at the 71st, 72nd, 73rd, 74th, and 75th cycle.

Acknowledgements
Financial support by the European M-ERA.NET 3 call (project9468 LaserBATMAN), Innovation Fund Denmark (grant number 1139-00001), and the Swedish Governmental Agency for Innovation Systems (Vinnova grant number 2022-01257).

Symbols

Symbol	Unit	Description
α	$[-]$	symmetry constant intercalation
β	$[-]$	symmetry constant degradation
ε_{SEI}	$[-]$	SEI layer porosity parameter
$\varepsilon_{S,p}$	$[-]$	Porosity cathode
δ_{SEI}	[m]	SEI layer thickness field, dependent variable
$\delta_{P,j}$	[m]	Particle radius
ρ_{SEI}	[kg m^{-3}]	density SEI layer
$\delta_{SEI,init}$	[m]	initial SEI layer thickness
κ_{SEI}	[Ω]	Electrical resistance SEI layer
$\eta_{int,j}$	[V]	intercalation overpotential
$\phi_{S,j}$	[V]	electrode potential field, dependent variable
$\phi_{E,j}$	[V]	electrolyte potential field, dependent variable
$\theta_{avg,j}$	$[-]$	Average particle saturation
$\theta_{max,p}$	$[-]$	Particle saturation max.
$\theta_{min,p}$	$[-]$	Particle saturation min.
$\mathcal{F}$	[C mol^{-1}]	Faraday's constant
$A_{int,j}$	[K]	Temperature dependency
$B_{eff,j}$	[K]	Temperature dependency
$c_{E,j}$	[mol m^{-3}]	Li-ion concentration, dependent variable
$c_{EC,P}$	[mol m^{-3}]	Solvent concentration in SEI layer field, dependent variable
$c_{EC,\infty}$	[mol m^{-3}]	EC concentration in solvent
$c_{EC,surf}$	[mol m^{-3}]	Solvent concentration at particle surface
$c_{S,j}$	[mol m^{-3}]	Electrode concentration field, dependent variable
$c_{S,max,j}$	[mol m^{-3}]	Maximum Li-ion electrode loading
$c_{S,surf,j}$	[mol m^{-3}]	Surface electrode Li-ion concentration
c^{ref}	[mol m^{-3}]	1[mol m^{-3}] reference concentration.
$D_{EC,P}$	[m^{2}s^{-1}]	diffusion coefficient of solvent in SEI layer
$D_{eff,S,j,ref}$	[m^{2}s^{-1}]	diffusion coefficient at reference temperature
$i_{int,j}$	[A m^{-2}]	Current density intercalation
i_s	[A m^{-2}]	Current density SEI layer
$i_{tot,j}$	[A m^{-2}]	Current density total
$i_{int0,j}$	[A m^{-2}]	Current density reference intercalation
I_{1C}	[A]	Cell apparent current, 1C-Rate
$k_{f,s}$	[m s^{-1}]	SEI layer formation reaction rate constant
$k_{int,j,ref}$	[A m^{-2}]	rate constant at reference temperature
L_p	[m]	Length of cathode
M_{SEI}	[kg mol^{-1}]	Molecular mass of SEI layer
r	[m]	radial coordinate, independent variable
R	[J mol^{-1}K^{-1}]	Gas constant
R_f	[Ω]	cell resistance
t	[s]	time, independent variable
T	[K]	temperature
T_{ref}	[K]	Reference temperature
$U_{0,j}$	[V]	Half cell potential
j	-	Subscript for domain